applied sciences

MDPI

*Article*

# Electrochemical Degradation of Crystal Violet Using Ti/Pt/$SnO_2$ Electrode

**Rachid El Brychy [1], Mohamed Moutie Rguiti [1], Nadia Rhazzane [1], Moulay Driss Mellaoui [1], Khalid Abbiche [1], Mhamed Abali [2], Lahcen Bazzi [1], Mustapha Hilali [1], Souad El Issami [1], Karine Groenen-Serrano [3,*] and Hanane Zejli [1,*]**

1 Team of Chemistry Physic, Faculty of Sciences, Ibn Zohr University, Agadir 80000, Morocco; brychy30@gmail.com (R.E.B.); rguiti2008@gmail.com (M.M.R.); nadia.razane.21@gmail.com (N.R.); mellaouimoulaydriss@gmail.com (M.D.M.); abbiche@gmail.com (K.A.); bazzilahcen@gmail.com (L.B.); hilali.mustapha@gmail.com (M.H.); s.elissami19@gmail.com (S.E.I.)
2 Laboratory of Applied Chemistry and Environment, Department of Chemistry, Faculty of Science, University Ibn Zohr, BP. 8106, Agadir 80000, Morocco; mhmedabali@gmail.com
3 Laboratoire de Génie Chimique, CNRS, Université Paul Sabatier, 118, Route de Narbonne, CEDEX 9, 31062 Toulouse, France
* Correspondence: serrano@chimie.ups-tlse.fr (K.G.-S.); zejlih@yahoo.fr (H.Z.)

**Featured Application: Treatment at source of wastewater containing dyes.**

**Abstract:** Today, organic wastes (paints, pigments, etc.) are considered to be a major concern for the pollution of aqueous environments. Therefore, it is essential to find new methods to solve this problem. This research was conducted to study the use of electrochemical processes to remove organic pollutants (e.g., crystal violet (CV)) from aqueous solutions. The galvanostatic electrolysis of CV by the use of Ti/Pt/$SnO_2$ anode, were conducted in an electrochemical cell with 100 mL of solution using $Na_2SO_4$ and NaCl as supporting electrolyte, the effect of the important electrochemical parameters: current density (20–60 mA $cm^{-2}$), CV concentration (10–50 mg $L^{-1}$), sodium chloride concentration (0.01–0.1 g $L^{-1}$) and initial pH (2 to 10) on the efficiency of the electrochemical process was evaluated and optimized. The electrochemical treatment process of CV was monitored by the UV-visible spectrometry and the chemical oxygen demand (COD). After only 120 min, in a 0.01 mol $L^{-1}$ NaCl solution with a current density of 50 mA $cm^{-2}$ and a pH value of 7 containing 10 mg $L^{-1}$ CV, the CV removal efficiency can reach 100%, the COD removal efficiency is up to 80%. The process can therefore be considered as a suitable process for removing CV from coloured wastewater in the textile industries.

**Keywords:** crystal violet; electrochemical oxidation; COD removal; decolourisation; depollution; water treatment; $SnO_2$; chloride

check for updates

**Citation:** El Brychy, R.; Rguiti, M.M.; Rhazzane, N.; Mellaoui, M.D.; Abbiche, K.; Abali, M.; Bazzi, L.; Hilali, M.; El Issami, S.; Groenen-Serrano, K.; et al. Electrochemical Degradation of Crystal Violet Using Ti/Pt/$SnO_2$ Electrode. *Appl. Sci.* **2021**, *11*, 8401. https://doi.org/10.3390/app11188401

Academic Editor: Jorge J. Rodriguez-Chueca

Received: 16 July 2021
Accepted: 6 September 2021
Published: 10 September 2021

**Publisher's Note:** MDPI stays neutral with regard to jurisdictional claims in published maps and institutional affiliations.

**Copyright:** © 2021 by the authors. Licensee MDPI, Basel, Switzerland. This article is an open access article distributed under the terms and conditions of the Creative Commons Attribution (CC BY) license (https://creativecommons.org/licenses/by/4.0/).

## 1. Introduction

The protection of the environment and the problem of cleaning up contaminated water and soil require a rapid response worldwide. Pollution is often of agricultural or industrial origin because of the discharge of untreated effluents into the natural environment. The growth of industrial activities increases obviously the pollution sources [1–4]. The textile industry is one of the industrial poles, it produces an enormous quantity of waste loaded with non-biodegradable dye stuffs [5–8]. These discharges contribute to the degradation of the quality of surface water and groundwater by their harmful and toxic side effects [9–11]. Dyes, widely used in the textile industry, are widespread pollutants [12,13]. The annual world production of dyes is about $7 \times 10^5$ tons, of which 5–10% is discharged into water by the textile industry [14]. They can be carcinogenic and toxic and their intensive use in everyday life can have harmful consequences on the environment and food [15–17]. Most of the dyes used are synthetic products, with an often-complex molecular structure, which

makes them stable and difficult to degrade by conventional treatment processes [18,19]. Thus, the implementation of treatment means adapted to this type of pollution is necessary in order to reduce its impact on the ecosystem. However, preventive effluents from the textile and processing industries must be treated at source before discharge into the environment. There are several physical methods that can be used to treat polluted effluents such as coagulation, flocculation, membrane filtration, ion exchange, adsorption. The main disadvantage of these processes is that they create waste that must then be treated or incinerated. The advanced oxidation processes generate in-situ, of the strongest oxidant—the hydroxyl radical. This radical can be efficient but very often it requires the addition of chemical regents. Thanks to the electrochemical generation of hydroxyl radicals from water oxidation, the electro-oxidation process is promising because it can be used for all types of effluents, it is compatible with environmental applications because the electrode is the only reagent used [20–27]. The simplicity of the equipment and the ease of use, the low cost of construction, the absence of sludge production, the mineralization of pollutants and the progression of the reaction by the electron are among the advantages of the electro-oxidation process [28–31]. The electrochemical oxidation of species in aqueous solutions can be carried out either by the transfer of electrons or by the transfer of oxygen atoms; alternatively, both pathways can be taken simultaneously. Direct electrochemical oxidation is heterogeneous: electron exchange occurs between organic species and the electrocatalytic electrode surface. Indirect oxidation uses an electrogenerated mediator. Indeed, a strong oxidant is generated at the anode and reacts chemically with the organics. The action of this oxidant can either occur close to the electrode surface if the oxidant is very reactive and not stable (i) the case of hydroxyl radical electrogenerated by water oxidation (Equation (1)), or in the bulk if the oxidant is sufficiently stable to diffuse into the solution (the case of active chlorine).

$$M + H_2O \rightarrow M(HO^{\cdot}) + H^+ + e^- \quad (1)$$

The in-situ production of oxidants presents various advantages: (i) in certain cases, complete mineralization can be reached, and reuse of the solution can be considered; (ii) in other cases, the action of the oxidant overcomes the limitations of mass transfer for the treatment of dilute solutions.

The presence or the deliberate addition of $Cl^-$ in a solution to be treated by electrochemical oxidation can accelerate the process of organic matter degradation. Indeed, the organic matter can be oxidized at the electrode and also at the center of the solution by chemical reaction with the active chlorine. For example, Panizza et al. [32] compared the COD abatement and color removal for direct and indirect electrolysis of a methylene blue solution. It appeared that indirect electrolysis facilitates faster mineralization and discoloration of the solution. This is due to the strong bleaching properties of active chlorine and the indirect electrolysis allows to overcome the mass transfer limitations.

The mechanism of electrooxidation depends mainly on the electrocatalytic properties of the anodic material. As a matter of fact, since the refractory compounds oxidize at high potentials, an anode with a high-oxygen overpotential is required. Studies on electrochemical processes by oxidation for water treatment began in the 1970s. Progress was made thanks to the development of new electrode materials. Among electrode materials, platinum used as reference has the advantage to be stable, fairly available, genuine without requiring further processing. However, this material has a low efficiency in anodic oxidation and expensive. Boron doped diamond (BDD) has appeared with growing interest over the last 30 years. As a matter of fact, BDD anodes show unique properties: a high electrochemical window, excellent electrochemical stability, and chemical inertness in acid and caustic media. BDD electrodes allow the complete removal of the organic matter (mineralization) to be envisaged. However, the high manufacturing and operating costs of the material due to high energy consumption limit the development of this material on an industrial scale. Metal oxides and in particular the dimensionally stable anodes, DSA®, which were discovered in the 1980s are alternatives [33–35]. Lead dioxide has a high

oxygen evolution overpotential. This material is easy to elaborate, cheap and available. However, lead ions may be released into the solution [32].

Tin dioxide has the same advantages, including high oxygen evolution potential, ease of preparation and low cost and the absence of heavy metal contamination [36,37]. However, the application of tin dioxide anodes can be limited by major problems such as their very low stability (the operational life is generally less than 8 h), which makes these electrodes uncompetitive for applications [38]. Nowadays, in order to extend the electrode life, researchers usually doped noble metal oxides (with Pt, Ru or Ir), which have high corrosion resistance and stability, into the anodic coating of the titanium substrate [39].

In our laboratory, the same lead dioxide anode doped with Pt was used for previous numerous studies without decreasing performances. For each case this electrode showed high efficiencies in organic removal. Among them, Rguiti et al., used tin oxide to treat oil mill wastewater (OMW), 96% decolourisation and 73% COD reduction were reached [40]. Other works were carried out by Baddouh et al., the treatment of methylene blue, a 100% removal of colour and a percentage of 80.9% of COD were observed the treatment of Thiabendazole fungicide with a 73% COD removal [41].

The main objective of the work carried out within the framework of this project, is to use an electrode based on $Ti/Pt/SnO_2$ in view of its application for the depollution of organic effluent including dye: violet crystal (CV).

This study will first define the suitable operating conditions for the treatment of effluents in order to obtain decolorization and COD abatement. For this purpose, several operating parameters will be considered such as the nature and concentration of electrolyte, the initial pH, the applied intensity and the initial CV concentration. Then, the energy cost will be evaluated and compared to other studies which were performed using high oxygen overpotential materials for dye treatment.

## 2. Materials and Methods

### *2.1. Chemicals*

The reagents used are of analytical quality. They are sodium chloride and crystal violet supplied by Sigma Aldrich. In this work, we were interested in the study of the dye crystal violet (CV) belonging to the family of cationic (basic) dyes. CV is an organic compound of the raw formula $C_{25}N_3H_{30}Cl$ (Figure 1) soluble in water, with a molar mass equals to 407.979 g $mol^{-1}$, it is widely used as dye for food and textile industry [6,42–46]. CV was chosen as dye model for its high solubility and its absorbance by UV/Vis spectrometry.

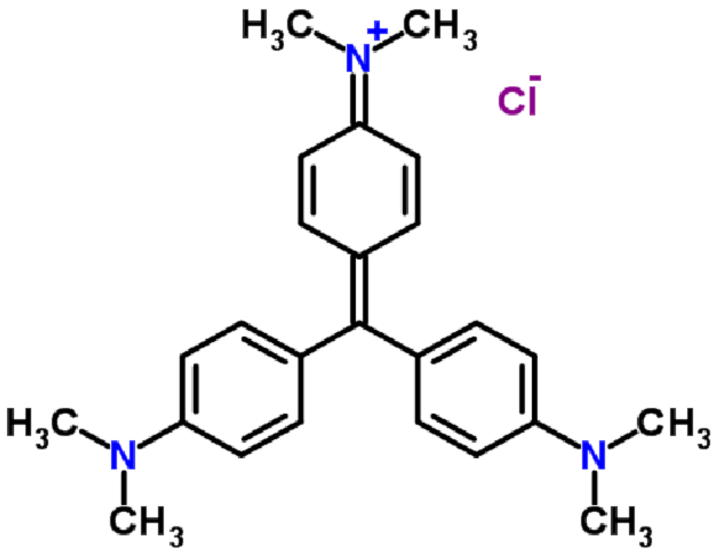


**Figure 1.** Structure of crystal violet (CV).

### *2.2. Electrochemical Cell and Method of Analysis*

All the electrochemical experiments (voltammetry and electrolysis) were carried out in an undivided and thermoregulated electrochemical cell of 200 mL and connected to a Versa studio type potentiostat/galvanostat. The electrochemical cell, shown in Figure 2, consists of a reference electrode ($Hg/Hg_2Cl_2/KCl$), a platinum wire as counter electrode and a working electrode (used as anode) of $Ti/Pt/SnO_2$ (mesh of 2 $cm^2$). The anode and cathode were positioned vertically and parallel to each other with a space between the electrodes of 1.5 cm.

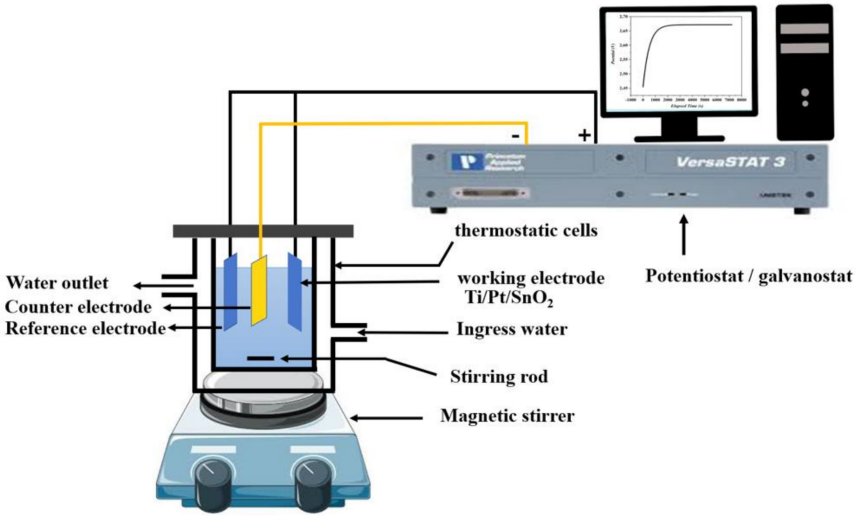


**Figure 2.** Schematic representation of the electrochemical cell.

In order to optimize the electrochemical treatment, different operating conditions have been tested: using $Na_2SO_4$ and NaCl as supporting electrolyte, the current density ranging from 20 to 60 mA $cm^{-2}$, CV concentration ranging from 10–50 mg $L^{-1}$, NaCl concentration (0.01–0.1 g $L^{-1}$) and initial pH ranging from 2 to 10.

The remaining concentration of CV is measured regurlarly by UV-visible spectrometry (Jenway 6705 UV-visible spectrophotometer) at 590 nm (wavelength accuracy ± 0.5 nm, accuracy ± 1% for absorbance up to).

The decolorization efficiency is calculated by using Equation (2):

$$CV\ removal\ rate\ (\%) = \frac{A_{0(590nm)} - A_{(590nm)}}{A_{0(590nm)}} \times 100 \quad (2)$$

with: $A_{0(590nm)}$: initial absorbance at λmax = 590 nm and $A_{0(590nm)}$: absorbance at λmax = 590 nm at time *t*.

The chemical oxygen demand (COD) was determined by photometric detection after adding the sample to a Lovibond® COD tube test and heating the sample for 2 h at 150 °C (uncertainty ± 3.5%).

The possible modifications of the surface conditions of the $Ti/Pt/SnO_2$ after use was analysed by scanning electron microscopy (Jeol JSM-6460LAV model) coupled to energy dispersive X-ray spectrometry. These analyses gave the surface morphology and the elemental composition of the formed species on the metal surface.

## 3. Results and Discussion

### *3.1. Cyclic Voltammetry*

A first electrochemical kinetic study is carried out to study the oxidation pathway of CV, namely if CV oxidation is performed by direct or indirect way. Cyclic voltammetry is the most used, simplest and fastest electrochemical technique for obtaining quantitative and qualitative information on any electroactive species. In these experiments, cyclic

voltammogram are obtained using a linear potential sweep to a working electrode at a constant sweep rate, first from a negative potential to a positive potential and then in the opposite direction.

Figure 3 shows a voltammogram obtained on a $Ti/Pt/SnO_2$ electrode in different electrolytes NaCl and/or $Na_2SO_4$ with and without CV.

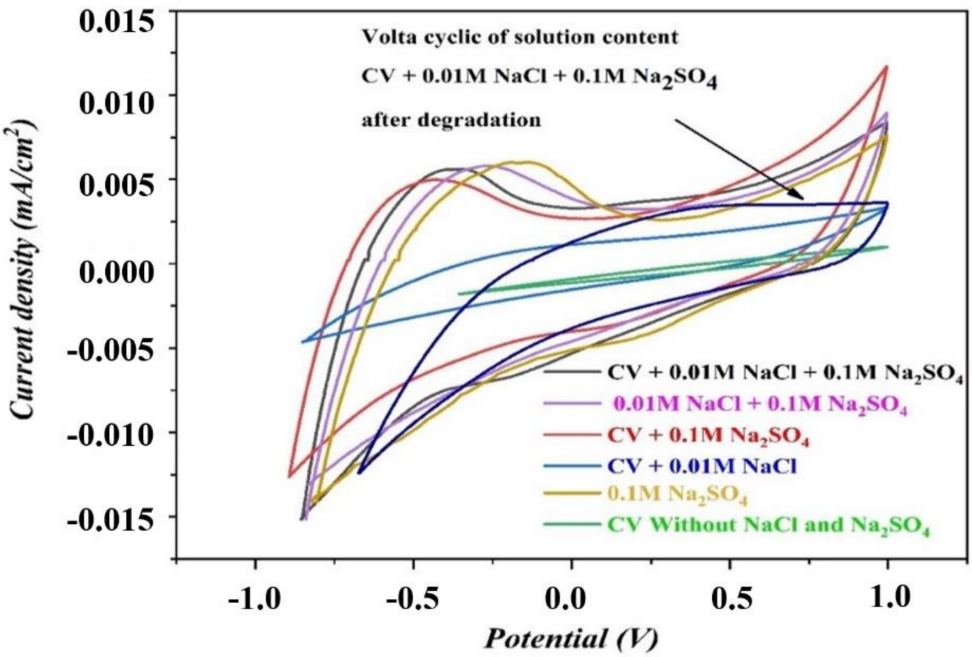


**Figure 3.** Cyclic voltammetry curve on an $Ti/Pt/SnO_2$ electrode, with a scan rate of 1 V $s^{-1}$.

The absence of electrolyte such as NaCl or $Na_2SO_4$ shows a low current during CV oxidation in a wide potential range. It is also observed that the voltammograms of CV solutions in an electrolyte is similar to the voltammogram obtained with the electrolyte alone. Therefore, these two findings highlight that CV does not oxidize directly at the electrode.

Moreover, the voltammogram obtained in a $Na_2SO_4$ solution shows a peak in oxidation (around −0.25 V/ref.) associated with a peak in reduction (around 0.25 V/ref.). These two peaks do not appear in the absence of $Na_2SO_4$. These peaks correspond to the oxidation of hydrogenosulfate ions to form sulfate radicals. These radicals are very reactive and not stable and form the peroxodisulfates ($S_2O_8{}^{2-}$) according to the respective Equations (3) and (4):

$$HSO_4^- + OH \rightarrow SO_4^- + H_2O \quad (3)$$

$$SO_4^- + HSO_4^- \rightarrow S_2O_8^{2-} + H^+ + e^- \quad (4)$$

In addition, one can observe that the voltammograms obtained with or without chloride ions are similar. Then the direct oxidation of chloride is not occurred.

Consequently, it is necessary to study the impact of the electrolyte used in the process on the dye removal.

One can note that whatever the electrolyte the general shape of the recorded voltammogram shows that the electrochemical reactions are not reversible. The use of a compartment separator for electrolysis is not required.

### *3.2. Influence of Operating Parameters*

#### 3.2.1. Effect of the Presence of Chloride Ions

The effect of the NaCl concentration on CV oxidation was studied under the following conditions, a concentration of 10 mg $L^{-1}$ CV, initial pH = 7 and at a current density of 50 mA $cm^{-2}$.

Figure 4a shows the temporal removal of CV using different concentrations of electrolytes ($Na_2SO_4$ and NaCl). It also appears that the initial rate of the CV removal (or decolorization) during electrochemical treatment is much higher as the NaCl concentration increases, due to the reactions between the generated chlorinated species and CV.

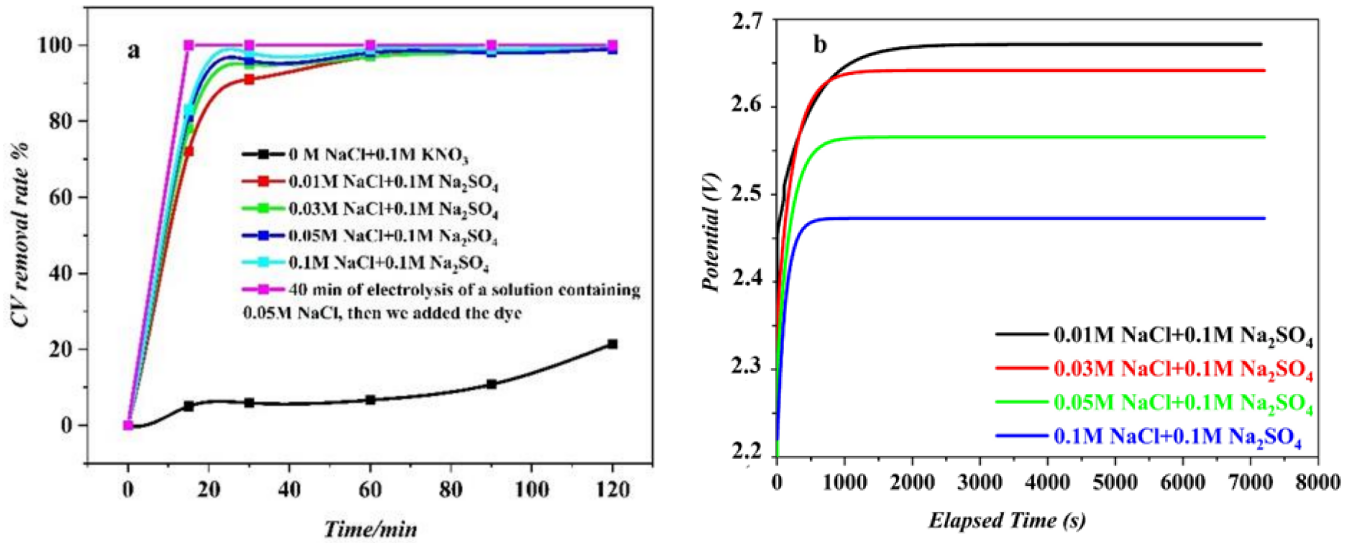


**Figure 4.** (**a**) Effect of NaCl concentration on degradation of the CV solution; (**b**) chronopotentiograms during electrolysis of the CV solution ($[CV]_0$ = 10 mg $L^{-1}$, initial pH = 7, i = 50 mA $cm^{-2}$ and temperature = 25 °C).

In fact, one can notice that after a 30 min treatment time, the rate reached a value of 91% for a sodium chloride concentration of 0.01 M NaCl + 0.1 M $Na_2SO_4$, 95% at 0.03 M NaCl + 0.1 M $Na_2SO_4$, 96% at 0.05 M NaCl + 0.1 M $Na_2SO_4$, and 98% for the 0.1 M NaCl + 0.1 M $Na_2SO_4$ concentration. However, after 2 h of treatment, a percentage of 100% was observed for the concentrations 0.01 M, 0.03 M, 0.05 M NaCl electrolyte.

However, in the absence of the latter, i.e., 0 M NaCl + 0.1 M $KNO_3$, the decolorization reaches only 16%. Chlorides can react with hydroxyl radicals at the anode to form hypochlorous acid or hypochlorite ions, depending on the pH, according to the Equations (5)–(7).

$$Cl^- + HO^{\cdot} \rightarrow ClO^- + H^+ + e^- \quad (5)$$

$$Cl^- + HO^{\cdot} \rightarrow HClO + e^- \quad (6)$$

$$HClO \rightarrow ClO^- + H^+ \quad (7)$$

A large amount of active chlorine in the solution due to the presence of chloride ions accelerated the indirect oxidation process of the wastewater loaded with organic matter and consequently the degradation process of the crystal violet dye was increased. A synergy of two processes takes place: oxidation by hydroxide radicals and oxidation by electrogenerated active chlorine

In order to evidence the CV degradation by active chlorine, the following experiment has been carried out: a solution containing only 0.05 M NaCl was prepared, and then this solution was electrolyzed during 40 min by applying a current density of 40 mA $cm^{-2}$, then the polarization was stopped and crystal violet was added and the absorbance was monitored over time. At the end, we noticed that the decolorization is almost total after only 30 min of electrolysis. The latter experience highlights that the main reaction to decolorize the solution is the chemical reaction between the active chlorine (generated electrochemically) and the CV.

In addition, Figure 4b shows that increasing the concentration of the electrolytes leads to a decrease in the operating voltage at the given current density and thus a decrease in the energy consumption.

3.2.2. Influence of Initial pH

The active chlorine can be in different forms depending on the pH. For that reason, the influence of pH on CV degradation was studied using different initial pH (2, 4, 7, 8, and 10), by adjusting the solutions to the desired values, using $H_2SO_4$ (1M) and NaOH (1M), while keeping constant the other operating conditions. The pH effect on the initial rate of CV decolorization as a function of time by imposing a current intensity i = 50 mA $cm^{-2}$ on the Ti/Pt/$SnO_2$ electrode in an aqueous solution of 10 mg $L^{-1}$ CV is shown in Figure 5. Samples are taken during the oxidation process and analyzed by UV-visible spectroscopy.

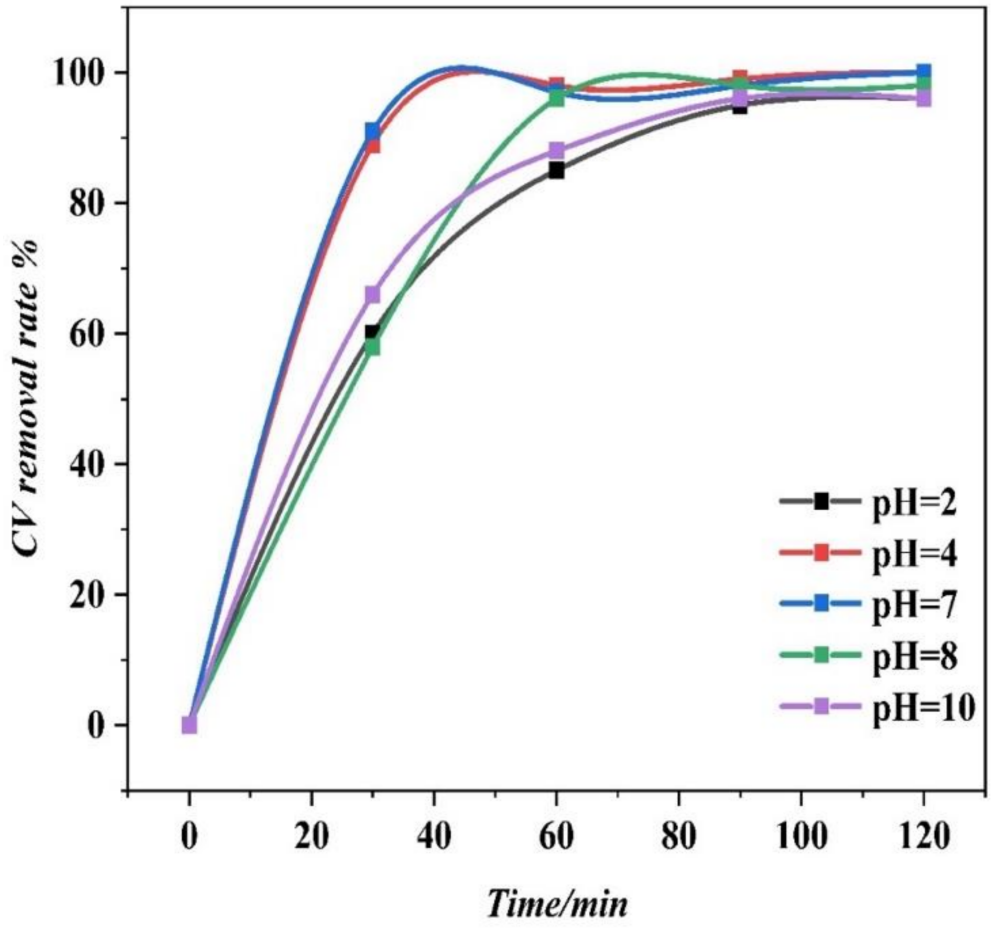


**Figure 5.** Effect of initial pH of CV removal ($[CV]_0$ = 10 mg $L^{-1}$, i = 50 mA $cm^{-2}$ and temperature = 25 °C).

It has been shown that after 30 min, a quasi-complete CV decolorization is reached at initial pH = 4 and at neutral pH. At more acidic pH (pH = 2) or basic (pH higher than 7) the rate of decolorization is lower (60% for pH = 2, 58% for pH = 8 and 66% for pH = 10). However, if the duration of the electrolysis is long enough, a quasi-decolorization of the solution is reached in the various cases.

In order to understand the differences depending on the pH value, a comparison of the CV removal rate with the preponderance diagram of the chlorinated species (Figure 6a [47]) was performed.

The results presented in Figure 6b were obtained as follows: each solution containing only the NaCl electrolyte and after adjusting the pH in the range 2–10, was electrolysed by applying a current density of 50 mA $cm^{-2}$ during 40 min, after stopping the polarization, the dye was added and stirred for 4 h. From these results, we observed that the decolorization is higher at pH = 4 and 7, because HClO is more stable. Therefore, from these results,

we can conclude that the species responsible for the oxidation of the organic matter is the form of HClO.

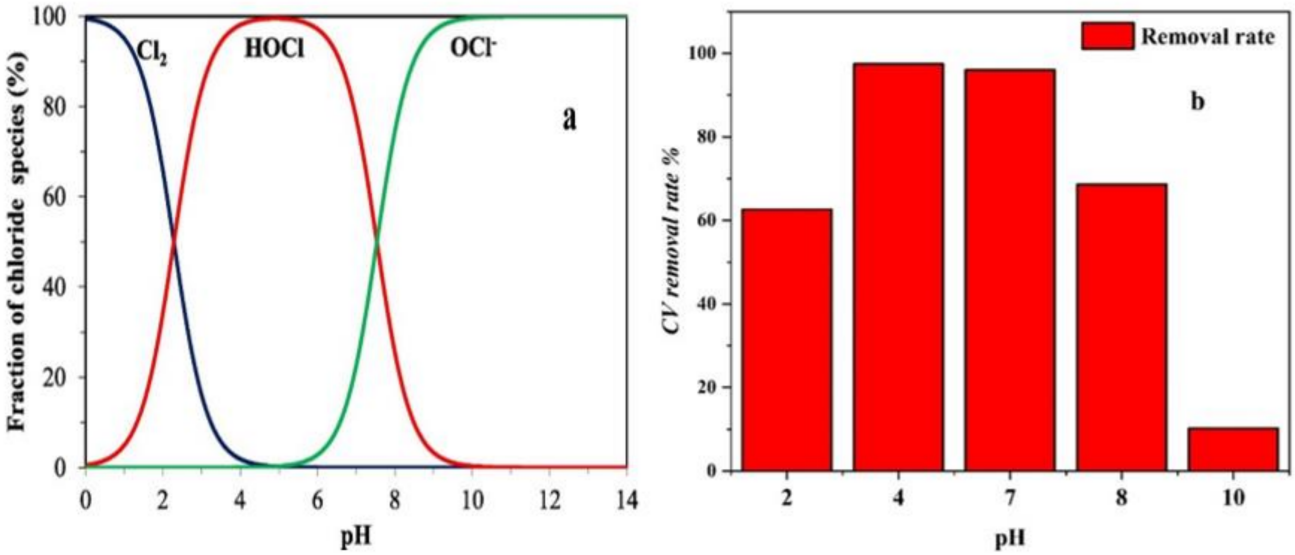


**Figure 6.** (**a**) Diagram of predominance of the chlorinated species [48]; (**b**) reduction of CV as a function of adjusted initial pH ($[CV]_0$ = 10 mg $L^{-1}$, i = 50 mA $cm^{-2}$ and temperature = 25 °C).

3.2.3. Influence of Applied Current

The effect of current density on CV degradation is studied by keeping the other parameters constant (initial CV concentration = 10 mg $L^{-1}$ and 50 mg $L^{-1}$ and initial pH = 7). The temporal variation of absorbance spectra in UV-vis for each of the current densities are shown in Suppl. Figures S1 and S2.

Figure 7a, shows the rate of CV degradation (10 mg $L^{-1}$). From these results it can be seen that the color removal increases significantly with increasing applied current density. When the current density increased from 20 mA $cm^{-2}$ to 60 mA $cm^{-2}$, the decolorization increased from 23% to 100%. On the other hand, with an initial CV concentration of 50 mg $L^{-1}$, it was found that when a current density of 50 mA $cm^{-2}$ and 60 mA $cm^{-2}$ was applied, a total reduction rate of 100% was achieved after 2 h of treatment.

The plot of CV removal as function of the applied current density for a given electrical charge, Figure 7c, shows that the increase of the applied current until 40 mA $cm^{-2}$ causes an increase of the quantity of electrogenerated HClO and also hydroxyl radicals. For a higher current, it is the amount of CV that limits the process.

Table 1 shows the velocity constants ($k$), half reaction times ($t_{1/2}$), the correlation coefficients ($R^2$). The values of the velocity constants were calculated from the linear regression of the corresponding semi-logarithmic curves according to a pseudo-first order reaction [49].

$$Ln\left(\frac{A_{0(590\,nm)}}{A_{t(590\,nm)}}\right) = k \times t \quad (8)$$

with $k$: the pseudo-first-order velocity constant ($min^{-1}$).

According to the results of Table 1, it is observed that the degradation of crystal violet dye for both concentrations 50 mg $L^{-1}$ and 10 mg $L^{-1}$ followed the pseudo-first order kinetics ($R^2 \geq 0.99$ in the range of i = 20 to 60 mA $cm^{-2}$).

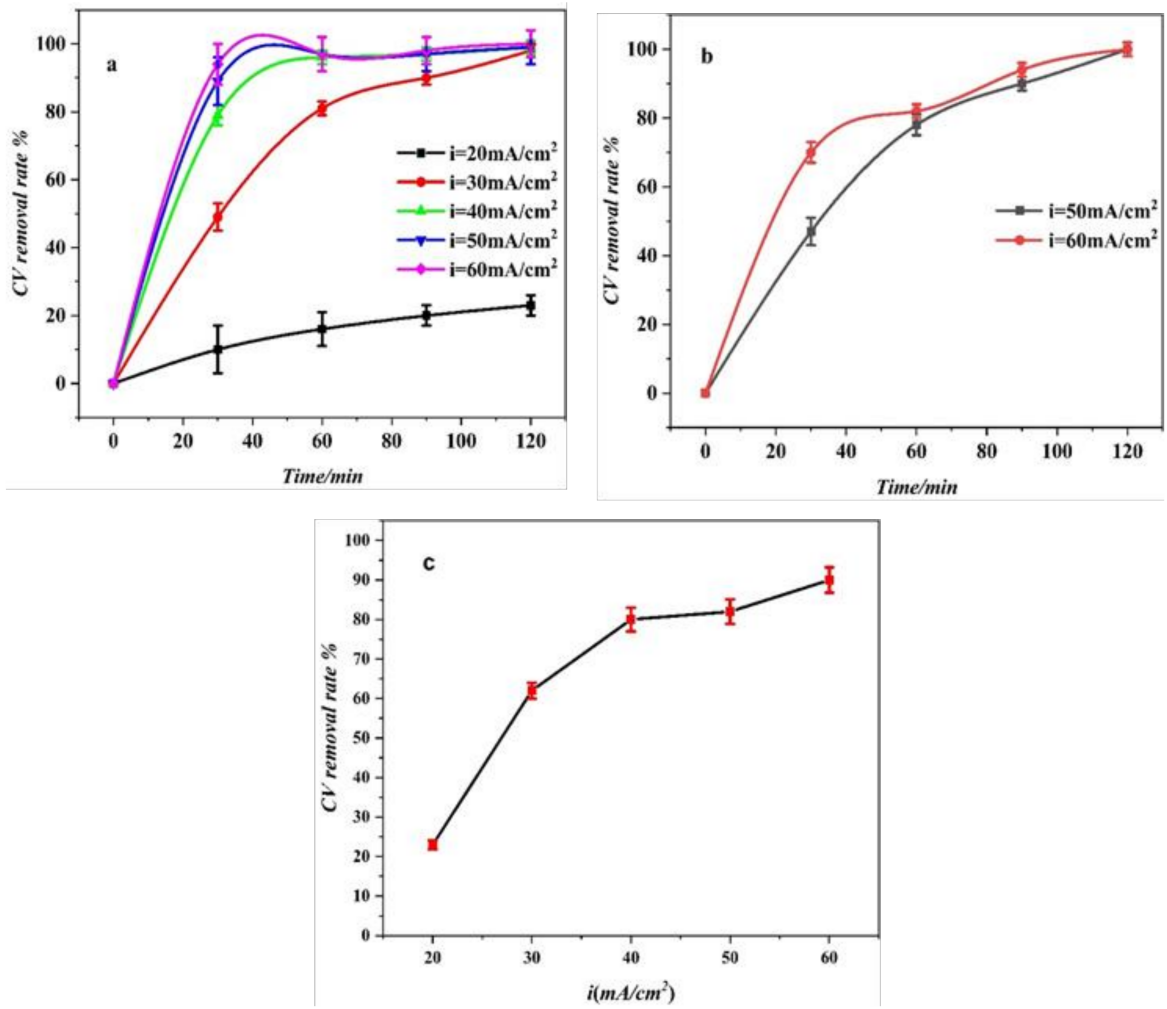


**Figure 7.** Effect of current density on efficiency of dye CV removal: $pH_0$ = 7, T = 25 °C (**a**) $[CV]_0$ = 10 mg $L^{-1}$; (**b**) $[CV]_0$ = 50 mg $L^{-1}$; (**c**) CV removal rate vs. current densities ($[CV]_0$ = 10 mg $L^{-1}$, initial pH = 7, temperature = 25 °C, Q = 7.2 C/$cm^2$).

**Table 1.** Kinetic parameters of the electrochemical degradation of the CV dye by means of a tin dioxide electrode.

| Initial CV Concentration | Current Density mA $cm^{-2}$ | Removal of CV (%) | Initial Rate Constant ($k \times 10^{-3}$ $min^{-1}$) | Half-Lives ($t_{\frac{1}{2}}$ min) | $R^2$ |
|---|---|---|---|---|---|
| 10 mg $L^{-1}$ | 20 | 23 | 3 | 245 | 0.9956 |
| | 30 | 98 | 28 | 25 | 0.9946 |
| | 40 | 99 | 53 | 13 | 0.9999 |
| | 50 | 100 | 56 | 12 | 0.9870 |
| | 60 | 100 | 60 | 12 | 1.0000 |
| 50 mg $L^{-1}$ | 50 | 100 | 25 | 28 | 0.9896 |
| | 60 | 100 | 29 | 24 | 0.9990 |

### 3.2.4. Influence of Initial CV Concentration

The initial concentration of the organic pollutant is a very important parameter in the treatment of polluted water [40,48]. The influence of this parameter in this electrochemical oxidation process is studied for both concentrations 10 and 50 mg $L^{-1}$ by setting the pH of the solution and the applied current to 50 and 60 mA $cm^{-2}$, respectively. The results presented in Figure 8a, show that at 60 min the CV disappearance is complete for the CV solution of 10 mg $L^{-1}$ whereas a 120 min treatment is required for the 50 mg $L^{-1}$ solution to reach the same percentage, i.e., a processing time only doubled for a concentration five times higher.

More specifically, Figure 8b highlights the CV abatement rate for the two initial concentrations as a function of the electrical charge in C/(mg $L^{-1}$) for 50 and 60 mA $cm^{-2}$. This comparison of the data highlights a perfect superposition of the values for both currents and that an electrical charge of 7 C (mg/L) is sufficient to remove more than 90% of the dye.

Therefore, it is necessary to adapt the applied electrical charge to render it as effective as possible.

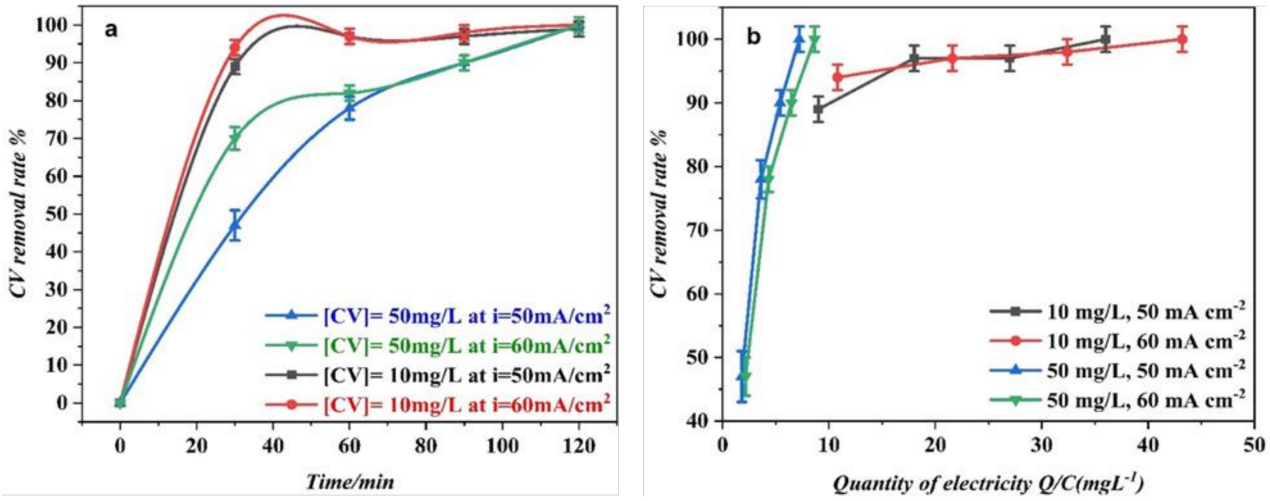


**Figure 8.** CV abatement rate as function of (**a**) time and (**b**) electrical charge in C/(mg$L^{-1}$). $[CV]_0$ = 10 mg $L^{-1}$, initial pH = 7, i = 50–60 mA $cm^{-2}$ and temperature = 25 °C.

### *3.3. Depollution in Terms of COD Removal and Current Efficiency (ICE)*

In order to study the potentialities of this electrode for depollution in terms of COD removal, electrolysis was carried out on a CV solution with an initial COD of 76 mg $L^{-1}$ at 50 mA $cm^{-2}$ and the electrolyte concentration (NaCl) was set at 0.01 M. Figure 9a shows the COD removal, calculated from Equation (9), as a function of electrolysis time using the Ti/Pt/$SnO_2$ anode.

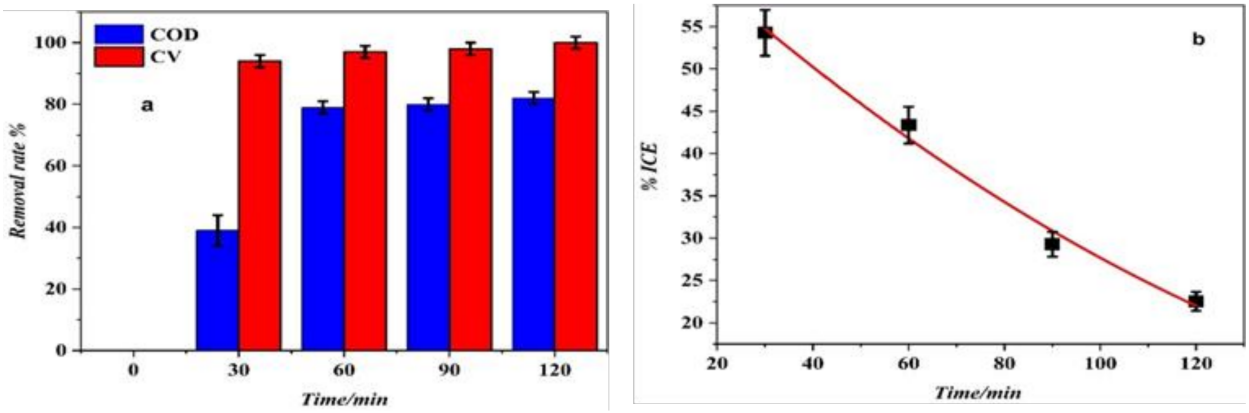


**Figure 9.** Temporal variation of COD and CV removal rate during electrolysis on Ti/Pt/$SnO_2$ anode. (**a**) Instantaneous current efficiency (**b**). Operating conditions: $[CV]_0$ = 10 mg $L^{-1}$, 50 mA $cm^{-2}$, initial pH = 7, temperature = 25 °C.

One can observe that the initial COD concentration of 76.41 mg $L^{-1}$ has been reduced to 9.16 mg $L^{-1}$ corresponding to an elimination of 82%. To detoxify the solution, the removal of the color is very often not sufficient. Indeed, 20 min of electrolysis are enough to reach the decolorization of the solution while there is still 60% COD. In these conditions,

it is useless to continue beyond one hour because a plateau has been reached in the COD removal.

Afterward, the instantaneous current efficiency (ICE) during crystal violet degradation process was calculated by the following Equation (10):

$$\%COD = \frac{COD_i - COD_t}{COD_i} \times 100 \quad (9)$$

$$\%ICE = FVs\frac{(COD_0 - COD_t)}{8I\Delta t} \times 100 \quad (10)$$

with $COD_i$: $COD$ value (mg $O_2$ $L^{-1}$) at the initial time, $COD_t$: $COD$ value (mg $O_2$ $L^{-1}$) at time $t$, both given (g $O_2$ $L^{-1}$); t is the time in ($s$); $F$ is the Faraday constant (96,487 C $mol^{-1}$); $V_s$ is the volume of the electrolyte (L); and $I$ is the current (A).

The ICE during the electrolysis is shown in Figure 9b. The initial value close to 55% confirms that the oxidation of the organic matter is not the only process. Indeed, part of the applied current used for the water discharge increases as the concentration of CV and by-products decreases. This exponential decrease is due to the limitation of mass transfer. To increase ICE values, an adjustment of the applied current must be done during the electrolysis.

### 3.4. Energy Consumption

In order to consider the industrialization of a process, it is useful to estimate the operating cost in terms of energy consumption (kW h $m^{-3}$) for the treatment of 1 $m^3$ of solution. The calculation of the energy consumed, expressed in W h $m^{-3}$ is determined from the following relation:

$$Energy\,consumption = \frac{(U \times I \times t)}{V_S} \quad (11)$$

where $U$ is the cell potential ($V$), $I$ is the applied current (A), t is the time of electrolysis (h), and $V_s$ is the volume of the treated solution ($m^3$). The price of electricity depends strongly on the country. For example, the unit price of electricity for industrial use is around 0.1346 € per kW h $m^{-3}$ in France and around 0.9010 Dh per kW h $m^{-3}$ in Morocco. Table 2 summarizes the process energy cost used in this study calculated at different treatment times: 30, 60, 90, 120 min. The treatment of 1 $m^3$ of CV under optimal treatment conditions ([NaCl] = 0.01 mol $L^{-1}$, [$Na_2SO_4$] = 0.1 mol $L^{-1}$ and i = 50 mA $cm^{-2}$) costs about 0.17 € (1.13 Moroccan dirham) for one hour of treatment. In these conditions, the electrochemical process allows to reach a maximum of CV removal higher than 95%.

On the other hand, Figure 10 shows the energy consumption as a function of removal for CV and COD. As expected, it can be noticed that the energy consumption increases significantly to reach the ceiling values of removal. Further, 97% decolorization and 79% COD removal are achieved after 60 min of treatment, i.e., an energy consumption of 1.26 kW h $m^{-3}$, while 2.52 kW h $m^{-3}$ (i.e., 120 min.) are needed to increase the CV and COD removal of 100% and 82%, respectively. As a result, electrochemistry can be used for the treatment of dyes. To render the process as economical as possible it is very important to establish specifications on the quality of the treated water in order to define stopping criteria.

**Table 2.** Energy requirements and costs for electrochemical treatment of solution containing CV at different time of treatment.

| I (mA) | Voltage U (V) | Time (min) | Energy Consumption (kW h $m^{-3}$) | Energy Cost (€) | CV Removal (%) |
|---|---|---|---|---|---|
| | | 30 | 0.215 | 0.029 | 49 |
| 20 | 2.15 | 60 | 0.430 | 0.058 | 81 |
| | | 90 | 0.645 | 0.087 | 90 |
| | | 120 | 0.860 | 0.116 | 98 |
| | | 30 | 0.337 | 0.045 | 79 |
| 30 | 2.25 | 60 | 0.675 | 0.091 | 96 |
| | | 90 | 1.012 | 0.136 | 97 |
| | | 120 | 1.350 | 0.182 | 99 |
| 40 | 2.42 | 30 | 0.484 | 0.065 | 89 |
| | | 60 | 0.968 | 0.130 | 97 |
| 50 | 2.52 | 30 | 0.630 | 0.085 | 94 |
| | | 60 | 1.260 | 0.170 | 97 |

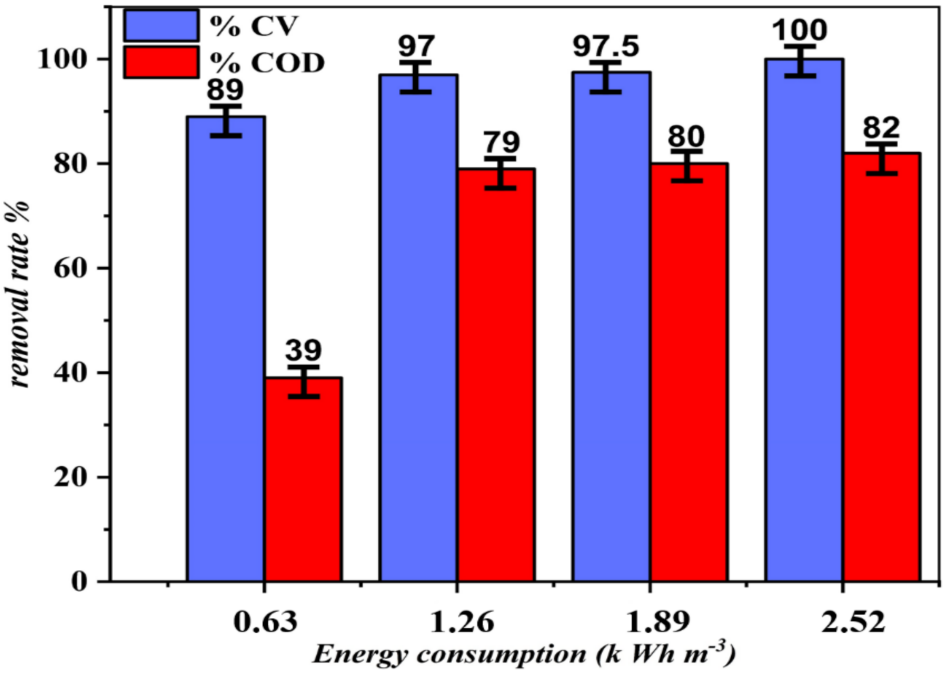


**Figure 10.** Evolution of decolorization and COD of CV dye as a function of energy consumption ($[CV]_0$ = 10 mg $L^{-1}$, 50 mA $cm^{-2}$, initial pH = 7, temperature = 25 °C).

### *3.5. Scanning Electron Microscopy (SEM)*

Scanning electron microscopy analysis were performed. It allows to highlight the changes that can occur on the surface of the Ti/Pt/$SnO_2$ electrode after its use for the treatment of solutions containing CV. Figure 11 shows the SEM images of the samples before and after use.

The comparison of Figure 11a,b evidences that the surface of the samples has been changed after use with the formation of a film on the Ti/Pt/$SnO_2$ electrode surface. To analyze the composition of the surface, EDX analysis, shown in Figure 12, were performed. The appearance of intense peaks attributed to the Ti, Pt, Sn elements on the EDX spectra shows that some part of the electrode substrate appear at initial state (before using) and the composition of O and C elements are higher after electrode use which reveal the adsorption of organics or polymer formation on the electrode surface.

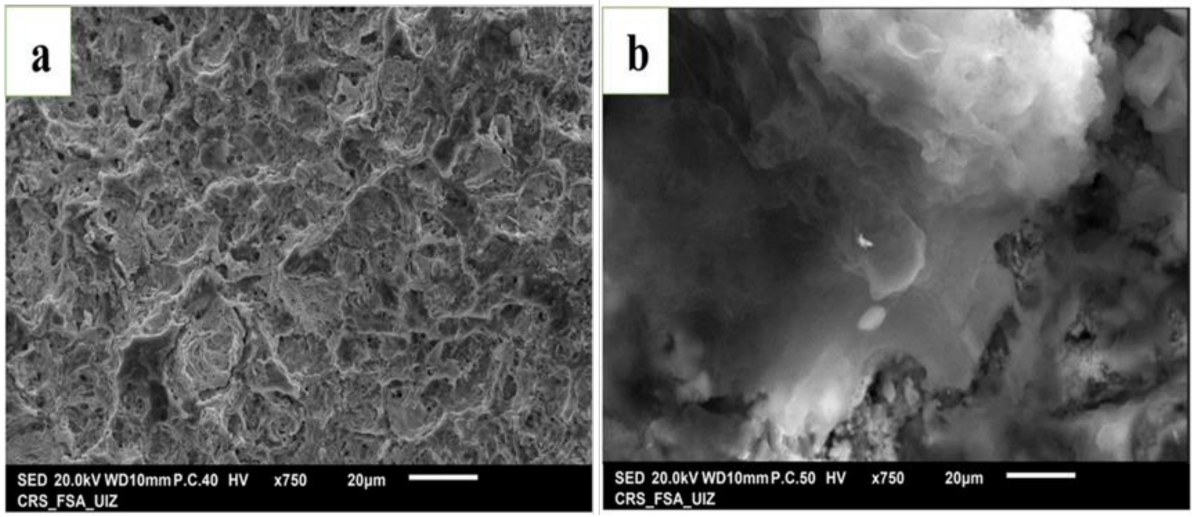


**Figure 11.** SEM images of the electrode surface before and after use: (**a**) Ti/Pt/$SnO_2$ surface before use, (**b**) Ti/Pt/$SnO_2$ surface after use.

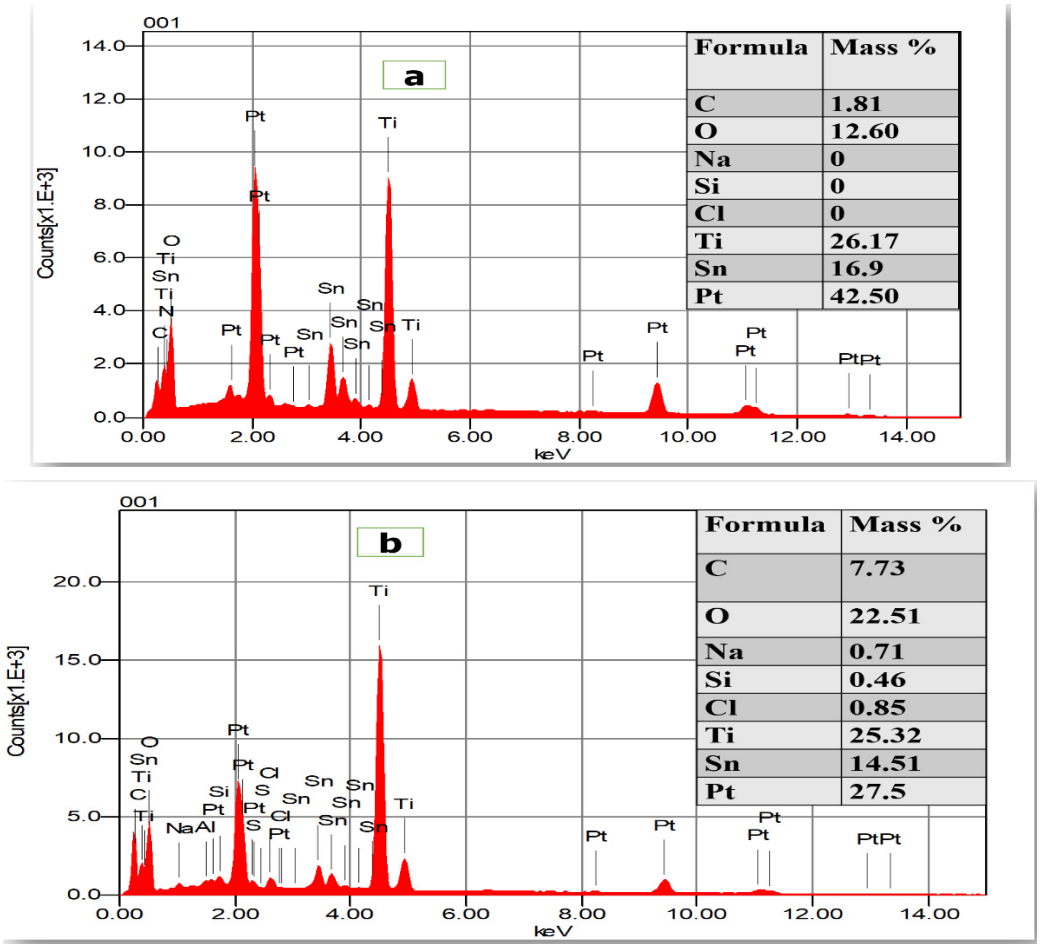


**Figure 12.** EDX analysis of the electrode surface before and after use: (**a**) Ti/Pt/$SnO_2$ surface before use, (**b**) Ti/Pt/$SnO_2$ surface after use.

The mapping images in Figure 13 show the distribution of chemical elements before and after the electrochemical CV treatment. Figure 13(1a,1b,2a,2b), reveal the presence and distribution of the mentioned elements in the nanocomposite, the distribution of oxygen

and carbon is more concentrated on the electrode surface Figure 13(2a,2b), due to the dye oxidation on the electrode surface during electrodeposition.

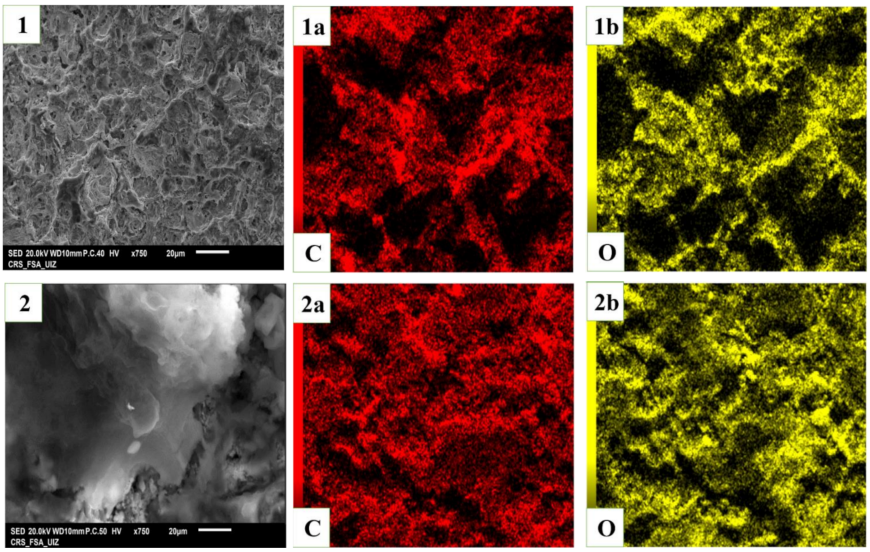


**Figure 13.** Elemental mapping images of Ti/Pt/$SnO_2$ electrode by SEM: (**1**) before electrolysis, (**2**) after electrolysis, (C: Carbon, O: Oxygen).

### *3.6. Comparative Study*

Table 3 lists the treatment of various dyes by anodic oxidation. It appears that even if the discoloration is generally complete, the COD abatement differs according to the operating conditions used. It can be seen that both BDD and $PbO_2$ anodes show good removals. As for the supporting electrolytes, $Na_2SO_4$ and NaCl are the most used. On one hand, $Na_2SO_4$ is usually chosen for the following reasons: (1) it is relatively cheap, (2) it can be oxidized to the strong oxidant $S_2O_8^{2-}$, and (3) it would not produce hazardous compounds during processing. On the other hand, a low concentration of NaCl is sufficient, of about a few mM. For electrochemical processes, the current density is one of the most important parameters. As shown in Table 3, in the range of 4 to 500 mA $cm^{-2}$, a higher current density could lead to a better treatment performance for the removal of pollutants, COD and TOC, i.e., removing the contaminants in less time or achieving a higher removal rate at the same time. For example, using malachite green as the model pollutant and G/β-$PbO_2$ as the anode, it would take 80 min for complete degradation, when the applied current density was 4 mA $cm^{-2}$ [50]. Similar findings could be observed for the degradation of purple blue on BDD, where the removal efficiency in COD was 82.61% and the current density was 500 mA $cm^{-2}$ [6]. In this work, with Ti/Pt/$SnO_2$, a COD removal of 80% was reached after 120 min of treatment at 50 mA $cm^{-2}$.

However, it is the comparison of energy consumption that highlights the interesting properties of $SnO_2$. Indeed, this electrode makes it possible to obtain great removals while maintaining a lower voltage than with the BDD for example. In addition, this material is cheaper than BDD and less toxic than $PbO_2$. For all these reasons, $SnO_2$ is a good material to treat organic pollutants.

**Table 3.** Degradation of different dyes by anodic oxidation.

| Pollutant | Electrodes | Current (mA $cm^{-2}$) | Electrolyte | Color Removal % | %COD | %TOC | Energy Consumption (kWh $m^{-3}$) | Ref. |
|---|---|---|---|---|---|---|---|---|
| Malachite green (MG) | G/β-$PbO_2$ | 4 | Phosphate buffer | 100 | 94 (80 min) | - | 7.4 | [50] |
| Acridine orange | Ce-$PbO_2$/$ZrO_2$ | 50 | 0.05 M $Na_2SO_4$ | 100 | - | 50 | 4.6 | [51] |
| Disperse Orange 29 | $PbO_2$ | 74 | 0.025 M NaCl | 100 | 100 (120 min) | - | 35 | [52] |
| Reactive red 141 | $PbO_2$ | 75 | 0.20 M NaCl | 100 | 100 (30 min) | - | 3.1 | [53] |
| Direct red 80 | Iron | 66 | 1 M $Na_2SO_4$ | 99 | 42 | - | 2.02 | [54] |
| | PPy | 2 | 1 M $Na_2SO_4$ | 100 | 46 | - | 5.46 | |
| | BDD | 2.5 | 1 M $Na_2SO_4$ | 100 | 76 | - | 14.7 | |
| Acid blue 22 | BDD | 20 | - | 100 | 27 (720 min) | - | 70 | [55] |
| Methyl red | $Ti/Ru_{0.3}Ti_{0.7}O_2$ | 60 | 0.003 M NaCl | - | 100 | 96 (360 min) | 67.05 | [56] |
| | Ti/Pt | 60 | 0.003 M NaCl | - | 100 | 83 (400 min) | 56.44 | |
| Purple blue | BDD | 500 | - | 94.3 | 82.61 | - | 11.9 KWh/Kg COD | [6] |
| Crystal violet | $Ti/TiO_2$ | 6.6 | 0.02 M NaCl | 66.27 | 83 (120 min) | - | - | [42] |
| | $Ti/TiO_2$-$RuO_2$ | 6.6 | 0.02 M NaCl | 90.96 | 92 (120 min) | - | - | |
| Crystal violet | Ti/Pt/$SnO_2$ | 50 | 0.1 M $Na_2SO_4$ + 0.01 M NaCl | 100 (120 min) | 82 | - | 2.5 | This work |

## 4. Conclusions

In conclusion, the results presented in this paper demonstrated that this crystal violet dye could be degraded and mineralized by the electrochemical process. On the other hand, the performance of this process could be optimized by varying the experimental parameters. Indeed, this study shows that the electrochemical degradation of CV using Ti/Pt/$SnO_2$ electrode is strongly influenced by current density, medium pH, NaCl concentration, initial dye concentration and treatment time. Electrolysis studies have shown that CV oxidation occurs through the synergy of hydroxyl radicals electrogenerated via water oxidation and active chlorine (HOCl) under galvanostatic conditions of 50 mA $cm^{-2}$ in 0.01 M NaCl and 0.1 M $Na_2SO_4$ and an initial neutral pH. Under these conditions, the process was able to effectively oxidize the initial dye completely without forming and accumulating by-products. It should be noted that the presence of a certain amount of chloride ions in the raw sewage was beneficial. On the contrary, if the wastewater does not contain chloride ions, then the addition of NaCl must be extremely controlled, that is, the compromise between the positive effect (i.e., improved degradation effect) and negative effects (i.e., shorter life of electrodes, corrosion of reactor and piping, etc.) but also the formation of undesired product such as organochlorides.

**Supplementary Materials:** The following are available online at https://www.mdpi.com/article/10.3390/app11188401/s1, Figure S1: UV/vis spectra of CV in electrochemical oxidation process on Ti/Pt/$SnO_2$ anode. Figure S2: The UV/vis spectra of CV in electrochemical oxidation process on Ti/Pt/$SnO_2$ anode with ($[CV]_0$ = 50 mg $L^{-1}$, initial pH = 7, temperature = 25 °C) at different of current density.

**Author Contributions:** Conceptualization, R.E.B., M.M.R., H.Z. and K.G.-S.; methodology, M.H., S.E.I.; software, M.A.; Formal analysis, M.D.M., K.A. and N.R.; Data curation, writing—original draft preparation, R.E.B. and M.M.R.; Writing-review and editing, K.G.-S. and H.Z.; visualization, M.H.; Supervision, L.B.; Project administration, K.G.-S. All authors have read and agreed to the published version of the manuscript.

**Funding:** This research received no external funding.

**Institutional Review Board Statement:** Not applicable.

**Informed Consent Statement:** Not applicable.

**Data Availability Statement:** Not applicable.

**Conflicts of Interest:** The authors declare no conflict of interest.

## References


1. Pillai, I.M.S.; Gupta, A.K.; Sahoo, C. Electrochemical oxidation of crystal violet dye (basic violet 3) using lead oxide electrodes. In Proceedings of the IASTED International Conference Environmental Management and Engineering (EME 2011), Calgary, AB, Canada, 4–6 July 2011; pp. 4–6.
2. Campos, A.M.; Riaño, P.F.; Lugo, D.L.; Barriga, J.A.; Celis, C.A.; Moreno, S.; Pérez, A. Degradation of crystal violet by Catalytic Wet Peroxide Oxidation (CWPO) with mixed Mn/Cu oxides. *Catalysts* **2019**, *9*, 530. [CrossRef]
3. Panizza, M.; Cerisola, G. Direct and mediated anodic oxidation of organic pollutants. *Chem. Rev.* **2009**, *109*, 6541–6569. [CrossRef] [PubMed]
4. Martínez-Huitle, C.A.; Rodrigo, M.A.; Sires, I.; Scialdone, O. Single and coupled electrochemical processes and reactors for the abatement of organic water pollutants: A critical review. *Chem. Rev.* **2015**, *115*, 13362–13407. [CrossRef] [PubMed]
5. Ersever, I.; Ravindran, V.; Tsai, H.-H.; Pirbazari, M. Modeling and design of anaerobic fluidized bed reactor with recycling for denitrification of reverse osmosis concentrates. *Chem. Eng. Sci.* **2014**, *108*, 111–122. [CrossRef]
6. Basha, C.A.; Sendhil, J.; Selvakumar, K.; Muniswaran, P.; Lee, C.W. Electrochemical degradation of textile dyeing industry effluent in batch and flow reactor systems. *Desalination* **2012**, *285*, 188–197. [CrossRef]
7. Bi, Q.; Guan, W.; Gao, Y.; Cui, Y.; Ma, S.; Xue, J. Study of the mechanisms underlying the effects of composite intermediate layers on the performance of Ti/$SnO_2$-Sb-La electrodes. *Electrochim. Acta* **2019**, *306*, 667–679. [CrossRef]
8. Palma-Goyes, R.E.; Silva-Agredo, J.; González, I.; Torres-Palma, R.A. Comparative degradation of indigo carmine by electrochemical oxidation and advanced oxidation processes. *Electrochim. Acta* **2014**, *140*, 427–433. [CrossRef]
9. Palma-Goyes, R.E.; Guzmán-Duque, F.L.; Peñuela, G.; González, I.; Nava, J.L.; Torres-Palma, R.A. Electrochemical degradation of crystal violet with BDD electrodes: Effect of electrochemical parameters and identification of organic by-products. *Chemosphere* **2010**, *81*, 26–32. [CrossRef]
10. Kaur, P.; Kushwaha, J.P.; Sangal, V.K. Evaluation and disposability study of actual textile wastewater treatment by electro-oxidation method using Ti/$RuO_2$ anode. *Process Saf. Environ. Prot.* **2017**, *111*, 13–22. [CrossRef]
11. Du, W.L.; Xu, Z.R.; Han, X.Y.; Xu, Y.L.; Miao, Z.G. Preparation, characterization and adsorption properties of chitosan nanoparticles for eosin Y as a model anionic dye. *J. Hazard. Mater.* **2008**, *153*, 152–156. [CrossRef]
12. Rangabhashiyam, S.; Anu, N.; Selvaraju, N. Sequestration of dye from textile industry wastewater using agricultural waste products as adsorbents. *J. Environ. Chem. Eng.* **2013**, *1*, 629–641. [CrossRef]
13. Moreira, F.C.; Boaventura, R.A.; Brillas, E.; Vilar, V.J. Electrochemical advanced oxidation processes: A review on their application to synthetic and real wastewaters. *Appl. Catal. B Environ.* **2017**, *202*, 217–261. [CrossRef]
14. Baghriche, O.; Djebbar, K.; Sehili, T. Etude cinétique de l'adsorption d'un colorant cationique (vert de méthyle) sur du charbon actif en milieu aqueux. *Sci. Technol. A Sci. Exactes* **2008**, 57–62.
15. Chanikya, P.; Nidheesh, P.; Babu, D.S.; Gopinath, A.; Kumar, M.S. Treatment of dyeing wastewater by combined sulfate radical based electrochemical advanced oxidation and electrocoagulation processes. *Sep. Purif. Technol.* **2021**, *254*, 117570. [CrossRef]
16. Chen, Y.; Baygents, J.C.; Farrell, J. Evaluating electrocoagulation and chemical coagulation for removing dissolved silica from high efficiency reverse osmosis (HERO) concentrate solutions. *J. Water Process Eng.* **2017**, *16*, 50–55. [CrossRef]
17. Alagesan, J.; Jaisankar, M.; Muthuramalingam, S.; Mousset, E.; Chellam, P.V. Influence of number of azo bonds and mass transport limitations towards the elimination capacity of continuous electrochemical process for the removal of textile industrial dyes. *Chemosphere* **2021**, *262*, 128381. [CrossRef] [PubMed]
18. Moreira, F.C.; Garcia-Segura, S.; Vilar, V.J.; Boaventura, R.A.; Brillas, E. Decolorization and mineralization of Sunset Yellow FCF azo dye by anodic oxidation, electro-Fenton, UVA photoelectro-Fenton and solar photoelectro-Fenton processes. *Appl. Catal. B Environ.* **2013**, *142*, 877–890. [CrossRef]
19. Weng, M.; Pei, J. Electrochemical oxidation of reverse osmosis concentrate using a novel electrode: Parameter optimization and kinetics study. *Desalination* **2016**, *399*, 21–28. [CrossRef]
20. Anglada, A.; Urtiaga, A.; Ortiz, I. Contributions of electrochemical oxidation to waste-water treatment: Fundamentals and review of applications. *J. Chem. Technol. Biotechnol.* **2009**, *84*, 1747–1755. [CrossRef]
21. Thiam, A.; Sirés, I.; Centellas, F.; Cabot, P.L.; Brillas, E. Decolorization and mineralization of Allura Red AC azo dye by solar photoelectro-Fenton: Identification of intermediates. *Chemosphere* **2015**, *136*, 1–8. [CrossRef]
22. Hamza, M.; Abdelhedi, R.; Brillas, E.; Sirés, I. Comparative electrochemical degradation of the triphenylmethane dye Methyl Violet with boron-doped diamond and Pt anodes. *J. Electroanal. Chem.* **2009**, *627*, 41–50. [CrossRef]
23. Kaur, P.; Sangal, V.K.; Kushwaha, J.P. Modeling and evaluation of electro-oxidation of dye wastewater using artificial neural networks. *RSC Adv.* **2015**, *5*, 34663–34671. [CrossRef]
24. Zhou, M.; Liu, L.; Jiao, Y.; Wang, Q.; Tan, Q. Treatment of high-salinity reverse osmosis concentrate by electrochemical oxidation on BDD and DSA electrodes. *Desalination* **2011**, *277*, 201–206. [CrossRef]
25. Singh, K.P.; Gupta, S.; Singh, A.K.; Sinha, S. Optimizing adsorption of crystal violet dye from water by magnetic nanocomposite using response surface modeling approach. *J. Hazard. Mater.* **2011**, *186*, 1462–1473. [CrossRef]
26. Jones, J.J.; Falkinham, J.O., III. Decolorization of malachite green and crystal violet by waterborne pathogenic mycobacteria. *Antimicrob. Agents Chemother.* **2003**, *47*, 2323–2326. [CrossRef]

27. Samarghandi, M.R.; Dargahi, A.; Shabanloo, A.; Nasab, H.Z.; Vaziri, Y.; Ansari, A. Electrochemical degradation of methylene blue dye using a graphite doped $PbO_2$ anode: Optimization of operational parameters, degradation pathway and improving the biodegradability of textile wastewater. *Arab. J. Chem.* **2020**, *13*, 6847–6864. [CrossRef]
28. Rahmani, A.R.; Shabanloo, A.; Fazlzadeh, M.; Poureshgh, Y. Investigation of operational parameters influencing in treatment of dye from water by electro-Fenton process. *Desalin. Water Treat.* **2016**, *57*, 24387–24394. [CrossRef]
29. Martínez-Huitle, C.A.; Panizza, M. Electrochemical oxidation of organic pollutants for wastewater treatment. *Curr. Opin. Electrochem.* **2018**, *11*, 62–71. [CrossRef]
30. Stirling, R.; Walker, W.S.; Westerhoff, P.; Garcia-Segura, S. Techno-economic analysis to identify key innovations required for electrochemical oxidation as point-of-use treatment systems. *Electrochim. Acta* **2020**, *338*, 135874. [CrossRef]
31. Souri, Z.; Ansari, A.; Nematollahi, D.; Mazloum-Ardakani, M. Electrocatalytic degradation of dibenzoazepine drugs by fluorine doped β-$PbO_2$ electrode: New insight into the electrochemical oxidation and mineralization mechanisms. *J. Electroanal. Chem.* **2020**, *862*, 114037. [CrossRef]
32. Panizza, M.; Barbucci, A.; Ricotti, R.; Cerisola, G. Electrochemical degradation of methylene blue. *Sep. Purif. Technol.* **2007**, *54*, 382–387. [CrossRef]
33. Kirk, D.; Sharifian, H.; Foulkes, F. Anodic oxidation of aniline for waste water treatment. *J. Appl. Electrochem.* **1985**, *15*, 285–292. [CrossRef]
34. Stucki, S.; Kötz, R.; Carcer, B.; Suter, W. Electrochemical waste water treatment using high overvoltage anodes Part II: Anode performance and applications. *J. Appl. Electrochem.* **1991**, *21*, 99–104. [CrossRef]
35. Trasatti, S. Electrocatalysis by oxides—Attempt at a unifying approach. *J. Electroanal. Chem. Interfacial Electrochem.* **1980**, *111*, 125–131. [CrossRef]
36. Adams, B.; Tian, M.; Chen, A. Design and electrochemical study of $SnO_2$-based mixed oxide electrodes. *Electrochim. Acta* **2009**, *54*, 1491–1498. [CrossRef]
37. Duan, Y.; Chen, Y.; Wen, Q.; Duan, T. Electrodeposition preparation of a cauliflower-like Sb–$SnO_2$ electrode from DMSO solution for electrochemical dye decolorization. *RSC Adv.* **2016**, *6*, 48043–48048. [CrossRef]
38. Jiang, Y.; Zhao, H.; Liang, J.; Yue, L.; Li, T.; Luo, Y.; Liu, Q.; Lu, S.; Asiri, A.M.; Gong, Z. Anodic oxidation for the degradation of organic pollutants: Anode materials, operating conditions and mechanisms. A mini review. *Electrochem. Commun.* **2021**, 106912. [CrossRef]
39. Zhang, G.; Huang, X.; Ma, J.; Wu, F.; Zhou, T. Ti/$RuO_2$-$IrO_2$-$SnO_2$ Anode for Electrochemical Degradation of Pollutants in Pharmaceutical Wastewater: Optimization and Degradation Performances. *Sustainability* **2021**, *13*, 126. [CrossRef]
40. Alcocer, S.; Picos, A.; Uribe, A.R.; Pérez, T.; Peralta-Hernández, J.M. Comparative study for degradation of industrial dyes by electrochemical advanced oxidation processes with BDD anode in a laboratory stirred tank reactor. *Chemosphere* **2018**, *205*, 682–689. [CrossRef]
41. Baddouh, A.; Rguiti, M.; Mohamed, E.; El Ibrahimi, B.; Bazzi, L.; Hilali, M. Electrochemical degradation of Thiabendazole fungicide by anodic oxidation on the tin oxide electrode ($SnO_2$). *Appl. J. Environ. Eng. Sci.* **2017**, *3*, 213–221.
42. Diouf, I.; Drogui, P.; Diop, E.H.; Lo, S.; Rumeau, M.; Mar Dop, C. Dégradation du cristal violet par électro-oxydation sur électrodes de Ti/$TiO_2$ et Ti/$TrO_2$-$RuO_2$: Étude de l'influence des paramètres opératoires sur l'efficacité du procédé. *Revue des Sciences de l'eau/J. Water Sci.* **2018**, *31*, 327–339. [CrossRef]
43. Caprarescu, S.; Miron, A.R.; Purcar, V.; Radu, A.L.; Sarbu, A.; Nicolae, C.A.; Pascu, M.; Ion-Ebrasu, D.; Raditoiu, V. Treatment of Crystal violet from synthetic solution using membranes doped with natural fruit extract. *CLEAN–Soil Air Water* **2018**, *46*, 1700413. [CrossRef]
44. Aysu, T.; Küçük, M. Removal of crystal violet and methylene blue from aqueous solutions by activated carbon prepared from Ferula orientalis. *Int. J. Environ. Sci. Technol.* **2015**, *12*, 2273–2284. [CrossRef]
45. Mbacké, M.K.; Kane, C.; Diallo, N.O.; Diop, C.M.; Chauvet, F.; Comtat, M.; Tzedakis, T. Electrocoagulation process applied on pollutants treatment-experimental optimization and fundamental investigation of the crystal violet dye removal. *J. Environ. Chem. Eng.* **2016**, *4*, 4001–4011. [CrossRef]
46. Pieczyńska, A.; Ossowski, T.; Bogdanowicz, R.; Siedlecka, E. Electrochemical degradation of textile dyes in a flow reactor: Effect of operating conditions and dyes chemical structure. *Int. J. Environ. Sci. Technol.* **2019**, *16*, 929–942. [CrossRef]
47. Deborde, M.; Von Gunten, U. Reactions of chlorine with inorganic and organic compounds during water treatment—Kinetics and mechanisms: A critical review. *Water Res.* **2008**, *42*, 13–51. [CrossRef]
48. Luna-Trujillo, M.; Palma-Goyes, R.; Vazquez-Arenas, J.; Manzo-Robledo, A. Formation of active chlorine species involving the higher oxide $MO_{x+1}$ on active Ti/$RuO_2$-$IrO_2$ anodes: A DEMS analysis. *J. Electroanal. Chem.* **2020**, *878*, 114661. [CrossRef]
49. Baddouh, A.; Bessegato, G.G.; Rguiti, M.M.; El Ibrahimi, B.; Bazzi, L.; Hilali, M.; Zanoni, M.V.B. Electrochemical decolorization of Rhodamine B dye: Influence of anode material, chloride concentration and current density. *J. Environ. Chem. Eng.* **2018**, *6*, 2041–2047. [CrossRef]
50. Ansari, A.; Nematollahi, D. A comprehensive study on the electrocatalytic degradation, electrochemical behavior and degradation mechanism of malachite green using electrodeposited nanostructured β-$PbO_2$ electrodes. *Water Res.* **2018**, *144*, 462–473. [CrossRef] [PubMed]

51. Yao, Y.; Ren, B.; Yang, Y.; Huang, C.; Li, M. Preparation and electrochemical treatment application of Ce-$PbO_2$/$ZrO_2$ composite electrode in the degradation of acridine orange by electrochemical advanced oxidation process. *J. Hazard. Mater.* **2019**, *361*, 141–151. [CrossRef] [PubMed]
52. Aquino, J.M.; Rocha-Filho, R.C.; Bocchi, N.; Biaggio, S.R. Electrochemical degradation of the Disperse Orange 29 dye on a β-$PbO_2$ anode assessed by the response surface methodology. *J. Environ. Chem. Eng.* **2013**, *1*, 954–961. [CrossRef]
53. Aquino, J.M.; Rocha-Filho, R.C.; Bocchi, N.; Biaggio, S.R. Electrochemical degradation of the reactive red 141 dye on a β-$PbO_2$ anode assessed by the response surface methodology. *J. Braz. Chem. Soc.* **2010**, *21*, 324–330. [CrossRef]
54. Lopes, A.; Martins, S.; Morao, A.; Magrinho, M.; Goncalves, I. Degradation of a textile dye CI Direct Red 80 by electrochemical processes. *Port. Electrochim. Acta* **2004**, *22*, 279–294. [CrossRef]
55. Panizza, M.; Cerisola, G. Removal of colour and COD from wastewater containing acid blue 22 by electrochemical oxidation. *J. Hazard. Mater.* **2008**, *153*, 83–88. [CrossRef] [PubMed]
56. Tavares, M.G.; da Silva, L.V.; Solano, A.M.S.; Tonholo, J.; Martínez-Huitle, C.A.; Zanta, C.L. Electrochemical oxidation of methyl red using Ti/$Ru_{0.3}Ti_{0.7}O_2$ and Ti/Pt anodes. *Chem. Eng. J.* **2012**, *204*, 141–150. [CrossRef]